

- [Ces13] J. Cesaratto *et al.*, Phys. Rev., **C88**, 065806 (2013).
- [Dec05] T. Decressin and C. Charbonnel, In *IAU Symp.*, volume 228, p. 395, 2005.
- [Dec07] T. Decressin *et al.*, Astron. Astrophys., **464**, 1029 (2007).
- [Den03] P. Denissenkov and F. Herwig, Astrophys. J. Lett., **590**, L99 (2003).
- [dM09] S. de Mink *et al.*, Astron. Astrophys. Lett., **507**, 1 (2009).
- [End90] P. M. Endt, Nucl. Phys., **A521**, 1 (1990).
- [Fir07] R. B. Firestone, Nucl. Data Sheets, **28**, 2319 (2007).
- [Gör89] J. Görres, M. Wiescher, and C. Rolfs, Astrophys. J., **343**, 365 (1989).
- [Gra12] R. G. Gratton, E. Carretta, and A. Bragaglia, Astron. Astrophys. Rev., **20**, 50 (2012).
- [Hal04] S. Hale *et al.*, Phys. Rev., **C70**, 045802 (2004).
- [Hig68] G. J. Highland and T. T. Thwaites, Nucl. Phys., **A109**, 163 (1968).
- [Ili10] C. Iliadis *et al.*, Nucl. Phys., **A841**, 31 (2010).
- [Kel17] K. J. Kelly *et al.*, Phys. Rev., **C95**, 015806 (2017).
- [Muk06] A. M. Mukhamedzhanov *et al.*, Phys. Rev., **C73**, 035806 (2006).
- [Pow99] D. C. Powell *et al.*, Nucl. Phys., **A660**, 349 (1999).
- [Rol75] C. Rolfs *et al.*, Nucl. Phys., **A241**, 460 (1975).
- [Sch83] P. Schmalbrock *et al.*, Nucl. Phys., **A398**, 279 (1983).
- [Ver88] W. J. Vermeer, D. M. Pringle, and I. F. Wright, Nucl. Phys., **A485**, 380 (1988).
- [Zys81] J. Zyskind, M. Rios, and C. Rolfs, Astrophys. J., **243**, L53 (1981), Erratum: 245, L97.

### 2.3.2 The Magnesium-Potassium Abundance Anomaly in Globular Clusters and Classical Novae

#### Project Abstract:

**Scientific Objectives:** The Mg-K abundance anomaly observed in the globular cluster NGC 2419 represents a major challenge for stellar evolution theory. By determining the rates of key reactions, we plan to gain insight into this puzzling phenomenon.

**Method:** We will perform direct measurements at LENA and particle transfer measurements at the Enge Split-pole Spectrograph. These will be complemented by nuclear structure measurements at HI $\gamma$ S. All three pieces of information will be important for determining the total rates of key reactions.

**Science Impact:** Obtaining improved rates for key reactions will lead to a better understanding of the history of matter in the early galaxy. It will help us understand the evolution of low mass stars and the role of classical novae in seeding the galaxy with products of nucleosynthesis.

**Personnel:**

**TUNL Faculty:** C. Iliadis(55%), R. Longland(25%), R.V.F. Janssens, A.E. Champagne

**Graduate Students:** David Gribble, NCSU student

**Postdocs/Research Scientists:** Postdoc to be hired in 2021

**Collaborators:** Jordi Jose (Barcelona), John Lattanzio (Monash University)

**Facilities:** LENA, HI $\gamma$ S, Tandem

**Major Resources:**  $\gamma\gamma$  coincidence spectrometer (at LENA); clover array (at HI $\gamma$ S); Split-pole Spectrograph

**Other Funding:** none

**1. Scientific Motivation**

Globular clusters are of paramount importance for testing theories of stellar evolution and early galaxy formation. Strong evidence for multiple populations of stars in globular clusters derives from observed abundance anomalies. The unexplained O-Na abundance anomaly, which appears in every globular cluster it was looked for, has already been discussed in Section 2.3.1. All we know is that this signature must have been produced in stars of a previous generation via hydrogen burning at temperatures near 75 MK [Pra07]. Here we will focus on an equally puzzling observation, the Mg-K anticorrelation in the globular cluster NGC 2419 [Coh12, Muc12]. The measurements imply that about 30% of all stars in this cluster consist of matter that underwent an unknown process.

In 2016, we performed reaction network simulations using the STARLIB library to study this phenomenon [Ili16]. Our specific goal was to constrain the burning temperature region that gave rise to the observations. We found that hydrogen burning temperatures of  $\approx 100$  MK to 120 MK are required, far higher than what is needed to produce the O-Na anomaly. Notice that supernovae in the early history of NGC 2419 are ruled out as an explanation. First, the metallicity of all observed stars in this cluster is constant, independent of the presence of the Mg-K signature. Second, the gravitational potential of the globular cluster is most likely insufficient to retain any supernova ejecta. We can also rule out massive and supermassive stars, and asymptotic giant branch (AGB) stars as polluter stars. Super-AGB stars could perhaps be viable candidates for the polluters only if stellar model parameters are fine-tuned to produce the required higher temperatures.

The only polluter candidates that can naturally provide the temperature-density conditions to produce the observed Mg-K anomaly are classical novae involving either CO or ONe accreting white dwarfs. However, one problem with this explanation is that almost all computed classical nova models assume the accretion of solar-metallicity matter, which is hardly conducive to the situation in NGC 2419, a cluster with a metallicity of two orders of magnitude below solar ( $[\text{Fe}/\text{H}] = -2.09 \pm 0.02$ ). We expect that the nucleosynthesis in low-metallicity novae will reach the mass region from silicon to calcium. Many key reaction rates in this region are uncertain precisely because classical nova models have so far completely disregarded this metallicity regime. Therefore, during the last grant cycle we started a campaign of measurements in this mass region.

**2. Accomplishments During the Last Grant Period**

We made progress on both the theoretical and experimental sides. Using the STARLIB library, we simulated the nucleosynthesis in globular clusters with special emphasis on the impact of key reaction rates. This work has been published in Ref. [Der17]. Figure 2.3–6 shows our simulated temperature-density conditions (blue dots) that reproduce the observations. The black lines represent evolutionary tracks for CO and ONe novae. The most important result of our work was that the spread in the blue dots is mainly caused by the rate uncertainties of the  $^{30}\text{Si}(p,\gamma)^{31}\text{P}$  and

$^{39}\text{K}(p,\gamma)^{40}\text{Ca}$  reactions. In our paper, we discussed each reaction and the nuclear quantities that need to be estimated to improve the rates.

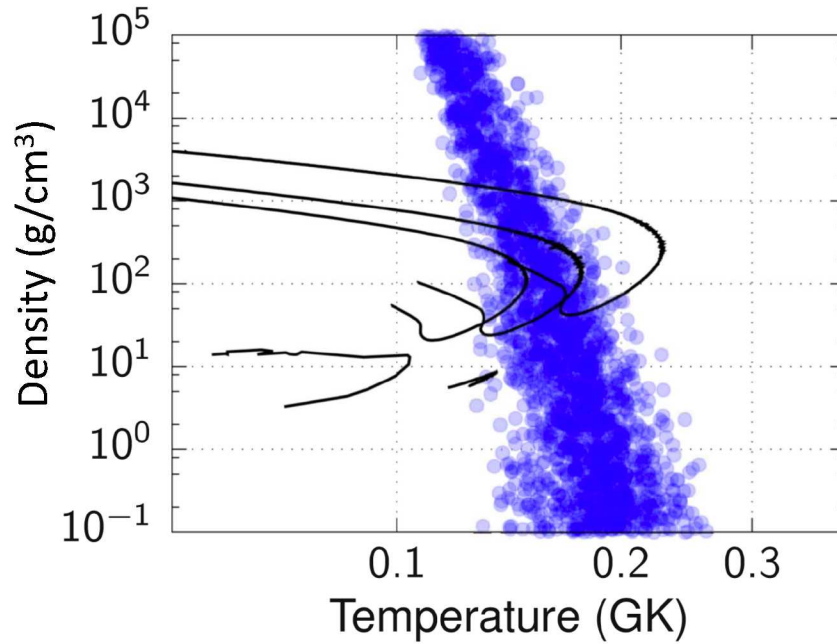


Figure 2.3-6: Temperature density conditions (blue dots) that reproduce the observed Mg-K abundance anomaly in NGC 2419. The results were obtained from reaction network simulations by randomly sampling all rates according to their individual probability densities. The superimposed black lines represent evolutionary tracks of classical nova models. Figure adopted from Ref. [Der17].

Subsequently, we evaluated new Monte Carlo reaction rates for the important  $^{39}\text{K}(p,\gamma)^{40}\text{Ca}$  reaction. This work was published in Ref. [Lon18]. We found that the rate is uncertain by at least an order of magnitude at astrophysically important temperatures from 100 MK to 200 MK. Figure 2.3-7 depicts the fractional resonance contributions to the total reaction rates. The widths of the bands indicate the fractional rate uncertainties. It can be seen that several low-energy resonances contribute to the total rate. The lowest-lying directly observed resonance occurs at  $E_{c.m.} = 606$  keV. It contributes to the total rate only at temperatures of  $> 300$  MK and is thus not important for hydrogen burning in globular clusters.

On the experimental side, we completed the measurement of the  $^{30}\text{Si}(p,\gamma)^{31}\text{P}$  reaction at LENA before the laboratory was dismantled. We observed a new low-lying resonance at 435 keV bombarding energy and improved the resonance strengths of higher-lying resonances. As a result, the total reaction rate has been lowered by one order of magnitude at temperatures important for NGC 2419 compared to the best previous prediction. This work has been published recently [Der20].

### 3. Project Description

#### (a) Nuclear Structure Measurements: $^{31}\text{P}(\gamma,\gamma')^{31}\text{P}$ and $^{40}\text{Ca}(\gamma,\gamma')^{40}\text{Ca}$

Despite our efforts described above, significant uncertainties remain in key reaction rates. When a resonance is directly observed, the quantum numbers of the corresponding compound levels are not important for calculating the reaction rate. But these rates also have contributions from unobserved

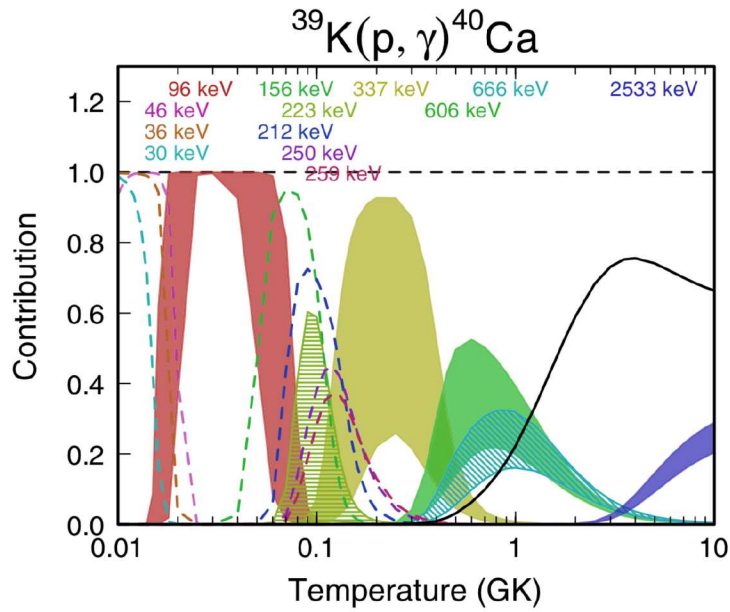


Figure 2.3-7: Fractional resonance contributions to the  $^{39}\text{K}(p,\gamma)^{40}\text{Ca}$  reaction rate. The resonance energies are given at the top. The widths of the bands indicate the uncertainties as predicted by our Monte Carlo rate simulation technique. Figure adopted from Ref. [Lon18].

resonances. In the latter case, the rate contribution must be estimated using nuclear structure information (spins, parities, partial widths, etc.). Nuclear Resonance Fluorescence experiments at HI $\gamma$ S represent an attractive possibility to determine the quantum numbers unambiguously. The reason is that the linearly polarized incident  $\gamma$  ray beam gives rise to an exceptionally strong alignment of the excited-level magnetic substates. As a result, the measured angular correlation between the incident and emitted  $\gamma$  rays allows for a straightforward determination of  $J^\pi$  values. We have submitted a manuscript for publication that presents angular correlations for all transitions of practical interest [Ili20].

Preliminary results from a test run at HI $\gamma$ S are shown in Figure 2.3-8. The spectrum was obtained with a linearly polarized beam from HI $\gamma$ S incident on a sample of natural calcium powder. The detector was located at an angle of  $90^\circ$  with respect to the beam direction. The two peaks indicated by the red flags show both photons from the  $8425 \rightarrow 3737 \rightarrow 0$  cascade in  $^{40}\text{Ca}$ . The 8425 keV level has an assigned spin-parity of  $2^-$  in ENSDF. Since the incident  $\gamma$  ray beam energy was  $\approx 8.4$  MeV, we must have directly populated this level. This, however, is unlikely because it would require an M2 transition. We will be able to determine unambiguously if the  $J^\pi$  value is  $2^+$  or  $2^-$ , because the measured angular correlation is very sensitive to this choice, as can be seen in the left part of Figure 2.3-8. These exploratory data are still being analyzed as part of a PhD thesis. As it happens, the 8425 keV level corresponds to the 96 keV resonance in  $^{39}\text{K}(p,\gamma)^{40}\text{Ca}$ , whose rate contribution is shown in Figure 2.3-7 as a brown band. Its rate contribution was estimated indirectly assuming a  $2^-$  assignment, implying a p-wave resonance. The rate contribution will change if the spin-parity turns out to be  $2^+$  (d-wave resonance).

The above discussion is an example for the important information that can be obtained at HI $\gamma$ S for improving reaction rate estimates. The data shown in Figure 2.3-8 were obtained during a test run that lasted a few days only. We are planning to remeasure the  $^{40}\text{Ca}(\gamma,\gamma')^{40}\text{Ca}$  reaction with the Clover array that will be commissioned soon. We are also planning similar measurements for



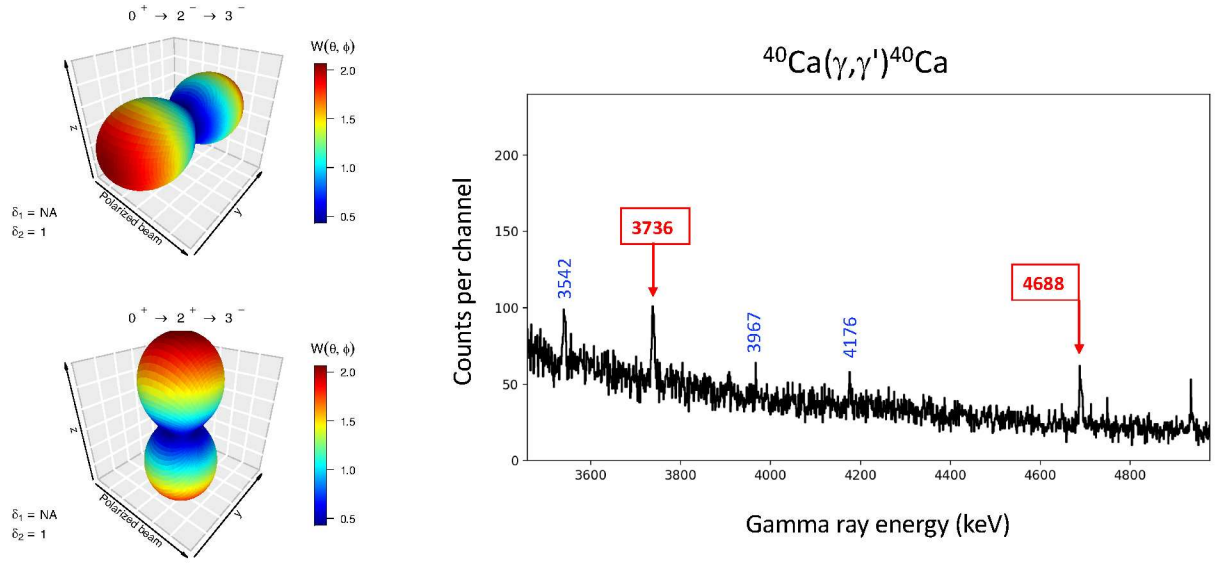


Figure 2.3-8: Preliminary results for  $^{40}\text{Ca}(\gamma, \gamma')^{40}\text{Ca}$ . (Left) Angular correlations for an incident linearly polarized  $\gamma$  ray beam and spin sequences of  $0^+ \rightarrow 2^- \rightarrow 3^-$  (top) and  $0^+ \rightarrow 2^+ \rightarrow 3^-$  (bottom). The incident  $\gamma$  ray beam moves along the positive x direction. (Right) Spectrum measured with a sample of natural calcium powder. The two red arrows show both photons from the  $8425 \rightarrow 3737 \rightarrow 0$  cascade in  $^{40}\text{Ca}$ .

$^{31}\text{P}(\gamma, \gamma')^{31}\text{P}$  to improve estimates of the  $^{30}\text{Si}(\text{p}, \gamma)^{31}\text{P}$  reaction rate. The data analysis for the latter measurement will be more challenging because of the  $^{31}\text{P}$  ground state spin-parity of  $1/2^+$ , which will give rise to  $\gamma$  ray transitions of mixed multipolarity. We are in the process of calculating the resulting angular correlation patterns [Ili20].

Estimating count rates for our planned HI $\gamma$ S measurements is challenging because the  $\gamma$  ray partial widths for the ground-state branches are not known. However, based on the statistics we collected during our test run, we estimate one week of running using the Clover array to complete the  $^{40}\text{Ca}(\gamma, \gamma')^{40}\text{Ca}$  measurement and two weeks of running to obtain important information for the  $^{31}\text{P}(\gamma, \gamma')^{31}\text{P}$  reaction. These measurements will form part of the thesis work of graduate student David Gribble.

### (b) Proton Transfer Reactions at the Enge Split-pole Spectrograph

The level structure of  $^{40}\text{Ca}$  close to the proton threshold is critical for determining the  $^{39}\text{K}(\text{p}, \gamma)^{40}\text{Ca}$  reaction rate. A number of important  $^{40}\text{Ca}$  levels are located too low in energy for a direct  $(\text{p}, \gamma)$  measurement and cannot be populated by Resonance Fluorescence because of unfavorable selection rules. Therefore, we are planning a complementary  $^{39}\text{K}(^3\text{He}, \text{d})^{40}\text{Ca}$  measurement at the Enge Split-pole spectrograph. This choice of reaction enables us to extract three key ingredients: (i) the energies of the excited states in the  $^{40}\text{Ca}$  compound nucleus, which correspond to  $(\text{p}, \gamma)$  resonances; (ii) the spin-parities of those states,  $J^\pi$ , that contribute most to the  $^{39}\text{K}(\text{p}, \gamma)^{40}\text{Ca}$  reaction rate; and (iii) the proton spectroscopic factors, which are used to calculate the partial widths and resonance strengths.

Our recent work in Ref. [Mar20] showed that the spectroscopic factors extracted from single-particle transfer reactions are poorly constrained unless the entrance and exit particle optical model potentials used to calculate the theoretical cross section are well known. We will continue this inves-

tigation by precisely measuring the entrance and exit channel elastic scattering cross sections for the  $^{39}\text{K}(^3\text{He},d)^{40}\text{Ca}$  reaction. With this information, we will be able to extract the potential parameters and their uncertainties that enter directly into the Distorted Wave Born Approximation (DWBA) analysis. A simultaneous treatment of all three channels in the reaction (elastic scattering in the entrance channel; elastic scattering in the exit channel; particle transfer cross section) will enable us to perform a full Bayesian analysis and will result in more realistic estimates for the spectroscopic factors. Furthermore, together with a reanalysis of previously measured transfer data in this mass region, we are planning to perform a local-global optical model analysis to further constrain the model parameters. We will investigate methods of building the computational infrastructure for performing these calculations in a consistent and user-friendly manner, and will make these computational tools available to the wider nuclear physics community. Such tools and techniques will become increasingly important for future particle transfer measurements at the Facility for Rare Isotope Beams (FRIB) and the SECAR recoil spectrometer.

Preliminary measurements of the  $^{39}\text{K}(^3\text{He},d)^{40}\text{Ca}$  reaction have already been completed at the TUNL Enge Split-pole Spectrograph. The spectrum collected at  $9^\circ$  is shown in Fig. 2.3–9. We populated a plethora of previously unresolved states in the astrophysically important region (shaded red). We plan to collect additional data to perform a full Markov Chain Monte Carlo analysis of the energies and proton partial widths of these states. These results are expected to strongly impact the  $^{39}\text{K}(p,\gamma)^{40}\text{Ca}$  reaction rate.

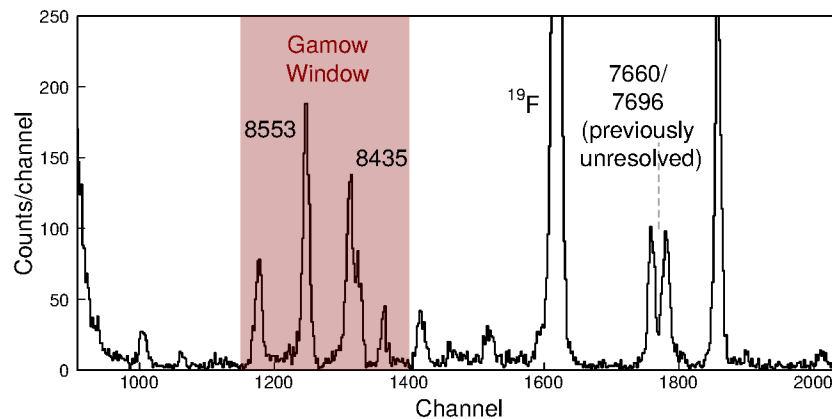


Figure 2.3–9: Preliminary results for the  $^{39}\text{K}(^3\text{He},d)^{40}\text{Ca}$  reaction measured at the TUNL Enge Split-pole Spectrograph. Of the 14 states observed in the spectrum, only four were previously known from proton transfer reactions. The two states at 7660 keV and 7696 keV were unresolved in previous  $(^3\text{He},d)$  studies [Set67]. The red shaded region highlights the states of astrophysical interest. Our new measurement of these states will impact the accuracy of the  $^{39}\text{K}(p,\gamma)^{40}\text{Ca}$  reaction rate.

The  $^{30}\text{Si}(^3\text{He},d)^{31}\text{P}$  reaction is also an important measurement for constraining the nucleosynthesis in globular clusters. This measurement was recently performed at Orsay, for which we produced the  $^{30}\text{Si}$  targets at TUNL. We are planning to perform additional measurements to better constrain the elastic scattering optical model parameters needed to interpret the transfer data. Furthermore, we are planning to measure  $^{31}\text{P}(d,d)^{31}\text{P}$  scattering, to constrain the exit channel optical model parameters. A Bayesian model will be developed in collaboration with the Orsay group to analyze the global data.

**(c) Direct Measurements at LENA:  $^{39}\text{K}(\text{p},\gamma)^{40}\text{Ca}$** 

About 20 levels appear in the  $^{40}\text{Ca}$  compound nucleus between the proton threshold and the lowest-lying observed resonance at a center-of-mass energy of 606 keV, as can be seen in Table II in Ref. [Lon18]. Figure 2.3–7 shows that below a stellar temperature of 200 MK, which is of main interest here, the total reaction rate is entirely dominated by unobserved resonances whose contributions had to be estimated from available nuclear structure information. We explained above that our planned  $^{40}\text{Ca}(\gamma,\gamma')^{40}\text{Ca}$  experiment at HI $\gamma$ S will hopefully improve our knowledge of the spin-parities of the threshold states. But it is also clear that we should be able to measure several  $^{39}\text{K}(\text{p},\gamma)^{40}\text{Ca}$  resonances directly at LENA. In fact, we expect that the main limitation of a direct measurements is neither related to the beam intensity nor the detection efficiency, but the stability of the potassium target. The previous measurement of Ref. [Kik90] tested KCl and K<sub>2</sub>SO<sub>4</sub> targets, which proved unsuitable, and settled on KI targets that could withstand a 30  $\mu\text{A}$  proton beam for 24 hours.

To estimate the count rates of our planned  $^{39}\text{K}(\text{p},\gamma)^{40}\text{Ca}$  measurements, we will assume a beam of only 30  $\mu\text{A}$ . We also assume the stoichiometry of KI for the target, a coincidence detection efficiency of 1%, and a branching ratio for the strongest transition (number of photons per resonance decay) of 10%. Under these assumptions we find an approximate count rate of  $4.5 \times 10^6 \omega\gamma$ , where  $\omega\gamma$  denotes the resonance strength in eV. The  $E_{c.m.} = 337$  keV resonance shown in Figure 2.3–7 has an upper limit of  $\omega\gamma \leq 3.7 \times 10^{-4}$  eV, which would yield  $\leq 1660$  counts per day. Since we will certainly be able to detect 1/10 of this count rate, we would reduce the current upper limit contribution of this level by one order of magnitude after one full day of running. Notice that none of our assumptions are overoptimistic: (i) the target will likely have a much more favorable stoichiometry (see Ref. [dM70] for conditioning KI targets to remove the iodine); (ii) our detection efficiency will likely be larger than 1%; (iii) we will run longer than just a single day; (iv) target development may result in potassium targets that could allow for a higher beam intensity (see our recent development work on the fabrication of implanted nanofoam targets [Hun19]). The background also needs to be considered. The decay scheme of  $^{40}\text{Ca}$  is interesting since most decays will likely feed the third and fourth excited states at 3737 keV and 3904 keV, respectively (the first excited state has a spin-parity of  $0^+$ ). The resulting secondary  $\gamma$  rays, or the primary  $\gamma$  rays feeding these low-lying levels, have energies much higher than the room background line from  $^{208}\text{Tl}$  and 2.614 MeV. Furthermore, the muon-induced background can be reduced by taking advantage of the pulsed beam at LENA.

A similar estimate for the much weaker  $E_{c.m.} = 250$  keV resonance (Figure 2.3–7) results in a count rate of 37 counts per day. If the true resonance strength is within an order of magnitude of its reported upper limit ( $\omega\gamma \leq 8.2 \times 10^{-6}$  eV [Lon18]) there is reasonable chance of a positive detection (or at least a significant reduction in its rate contribution). The two resonances at  $E_{c.m.} = 259$  keV and 305 keV have resonance strength upper limits between the values quoted above and we should be able to significantly improve their rate estimates as well. These measurements will form part of the thesis work of graduate student David Gribble.

---

[Coh12] J. G. Cohen and E. N. Kirby, *Astrophys. J.*, **760**, 86 (2012).

[Der17] J. R. Dermigny and C. Iliadis, *Astrophys. J.*, **848**, 14 (2017).

[Der20] J. Dermigny *et al.*, *Phys. Rev.*, **C102**, 014609 (2020).

[dM70] R. J. de Meijer *et al.*, *Nucl. Phys.*, **A155**, 109 (1970).

[Hun19] S. Hunt *et al.*, *Nucl. Instrum. Methods*, **A921**, 1 (2019).

[Ili16] C. Iliadis *et al.*, *Astrophys. J.*, **818**, 98 (2016).

- [Ili20] C. Iliadis and U. Friman-Gayer, Submitted, 2020.
- [Kik90] S. W. Kikstra *et al.*, Nucl. Phys., **A512**, 425 (1990).
- [Lon18] R. Longland, J. Dermigny, and C. Marshall, Phys. Rev., **C98**, 025802 (2018).
- [Mar20] C. Marshall *et al.*, *Bayesian Analysis of the  $^{70}\text{Zn}(d, ^3\text{He})^{69}\text{Cu}$  Transfer Reaction*, 2020, Accepted to Phys. Rev. C.
- [Muc12] A. Mucciarelli *et al.*, Mon. Not. R. Astron. Soc., **426**, 2889 (2012).
- [Pra07] N. Prantzos, C. Charbonnel, and C. Iliadis, Astron. Astrophys., **470**, 179 (2007).
- [Set67] K. K. Seth *et al.*, Phys. Rev., **164**, 1450 (1967).

### 2.3.3 Oxygen Isotopes in Asymptotic Giant Branch Stars

#### Project Abstract:

**Scientific Objectives:** Oxygen isotopic ratios can provide very detailed information about the stellar interior. At present, predictions of the  $^{16}\text{O}/^{17}\text{O}$  ratio are uncertain by about a factor of two, owing to a systematic disagreement amongst existing measurements of the  $^{17}\text{O}(\text{p},\alpha)^{14}\text{N}$  reaction. There is also a factor of 10 disagreement in  $^{18}\text{O}$  synthesis arising from experimental inconsistencies between measurements of the  $^{18}\text{O}(\text{p},\alpha)^{15}\text{N}$  reaction. Our goal is to resolve these discrepancies, permitting more precise calculations of the stellar  $^{17}\text{O}/^{16}\text{O}$  and  $^{18}\text{O}/^{16}\text{O}$  ratios.

**Method:** The key resonance in the  $^{17}\text{O}(\text{p},\alpha)^{14}\text{N}$  reaction is at  $E_{cm} = 65.5$  keV. In the  $^{18}\text{O}(\text{p},\alpha)^{15}\text{N}$  reaction, the key resonance is at  $E_{cm} = 90$  keV. We plan to measure these reactions using the LENA facility, which produces the most intense proton beams available at these energies.

**Science Impact:** Improved reaction rates for  $^{17}\text{O}(\text{p},\alpha)^{14}\text{N}$  and  $^{18}\text{O}(\text{p},\alpha)^{15}\text{N}$ , which will be important for interpreting observations of asymptotic giant branch stars and abundance trends in pre-solar grains.

#### Personnel:

**TUNL Faculty:** A.E. Champagne (35%), R. Longland (15%), C. Iliadis (15%).

**Graduate Students:** Clay Wegner

**Postdocs/Research Scientists:** A. Lauer, Postdoc to be hired in 2021.

**Collaborators:**

**Facilities:** Laboratory for Experimental Nuclear Astrophysics (LENA)

**Major Resources:** LENA ECR accelerator, particle detector array.

**Other Funding:** none

#### 1. Scientific Motivation

Oxygen isotopic ratios are very sensitive to stellar temperature and thus can provide detailed information about the stellar interior. The most precise measurements of oxygen abundances come from pre-solar grains, but here the challenge is matching grains to particular production sites. However, it is also possible to measure oxygen isotopes in stellar atmospheres (one of the few elements where it is possible to obtain isotopic information from stellar spectra). A review of oxygen isotopes as